Urban change monitoring from multi-temporal TerraSAR-X images

Wen Liu and Fumio Yamazaki
Department of Urban Environment Systems
Chiba University
Chiba, Japan
Wen_liu@graduate.chiba-u.jp

Abstract—**Monitoring urban growth and change is an important issue for urban planning and disaster management. In this study, three temporal TerraSAR-X images are used to monitor the urban changes. The difference and correlation coefficient between two images are calculated with a sliding window. Then a new factor that composites the difference and correlation coefficient is proposed to detect the changes. The Tokyo international airport expansion construction is used as a case study. The urban changes due to the progress of the construction are detected by the proposed approach. Then an aerial photograph taken during the construction and the visually detected results are used to verify the accuracy of the results.**

I. INTRODUCTION

Urban areas grow and change rapidly all over the world. Monitoring urban areas has become an increasingly important topic. Regular and up-to-date information on urban changes is required for strategic city planning purposes, environmental impact assessment, and for the appropriate allocation of services and infrastructure within towns and cities [1-2]. Current approaches to urban monitoring generally involve ground surveys and interpretation of aerial photographs. The improvement of remote sensing technology makes satellite images an efficient method to collect urban information. Compared to optical sensors, synthetic aperture radar (SAR) does not suffer from the limitations of weather condition. Also the side-looking system of SAR sensors can obtain the 3D information of urban areas. The high resolution of SAR images (ALOS/PALSAR and TerraSAR-X) is well suited for urban applications, e.g. urban modeling as well as for damage mapping after disasters.

Urban areas are generally characterized by high SAR backscattering intensities due to the predominance of single- and double-bounce backscattering [3]. The previous studies on the use of multi-temporal SAR data for change detection have achieved some promising results [4-5]. These studies focused on using ERS interferometric coherence data to detect the land cover changes in urban areas. However, the complex coherence obtained from the interferometric analysis is sensitive to satellite geometry, acquisition duration and wavelengths of radar [6]. Additionally, TerraSAR-X imagery has higher resolution (1.25 m) to detect more details, e.g. a single building change. Matsuoka and Yamazaki [7] developed an automated method to detect hard-hit areas in the 1995 Kobe Earthquake, using the backscattering coefficient difference and the correlation coefficient between pre- and post-event ERS images. The backscattering coefficient provided as the amplitude information is less dependent on the above-motioned conditions for interferometric analysis [8]. Therefore, this method also can be used to monitor urban changes in case of high-resolution TerraSAR-X images.

In this study, three TerraSAR-X images of Tokyo International Airport are used to monitor urban changes by an improvement method proposed in the reference [7]. The results of change detection are compared with an aerial photograph and visual inspection results, to verify the accuracy.

II. STUDY AREA AND DATA

The study area focuses on Tokyo International Airport (commonly known as Haneda Airport), Japan, shown in Fig. 1. Tokyo International Airport (HND) is one of the two primary airports serving the Tokyo area, handling almost all domestic flights. It has now three runways, two domestic passenger terminals and a temporary international terminal. Since international service has expanded significantly in recent years, the Japanese government plans to expand HND's international role in the future. Hence, the third terminal for international flights and a new runway, which is called D-runway, is under construction from 2007. By the completion of the D-runway and the new terminal building, take-off and landing counts will drastically increase from 296 thousands to 407 thousands a year, 1.4 times more flights than now. This project has a great impact in both economy and urban development [9].

Three TerraSAR-X images taken in different days during 2008 to 2009 were used to monitor the progress of this construction, shown in Fig. 2(a-c). The first image was taken on May 23th, 2008 (UTC) with 42.82° incidence angle, the second one was taken on October 10th, 2008 with 42.83° incidence angle, and the third one was taken on November 23th, 2009 with 42.81° incidence angle at the center. All the images were taken by HH polarization, and in the descending path. Since they were taken in StripMap Mode [10], the resolution was about 3.3 m. After the enhanced ellipsoid correction (EEC), three images were transformed into 1.25 m/pixel. The images include about 46.88 km^2 areas.

978-1-4244-8657-1/11/$26.00 ©2011 IEEE

At the right-upper part of the three TerraSAR-X images, a shape which is similar to the steel-jacket-platforms part of D-runway can be seen. This phenomenon, known as "ambiguity", occurs due to the low pulse repetition frequency (PRF). There are the significant returns from targets have the same Doppler history as the signal, then these targets appear as if illuminated by apportion of the physical antenna beam away from the antenna boresight in azimuth [11].

III. IMAGE PREPROCESSING

Before the change detection, a radiometric calibration and a speckle filtering approaches were applied on the three TerraSAR-X images. The radiometric calibration approach can transform the digital number in the SAR image to the Sigma Naught (σ^0), which represents the radar reflectivity per unit area in the ground range. According to Infoterra [12], the Sigma Naught of TerraSAR-X images can be calculated by (1).

$$\sigma^0 = 10 \cdot \log_{10}(k_s \cdot |DN|^2) + 10 \cdot \log(\sin \theta_{loc}) \quad (1)$$

where k_s is the calibration factor, which can be found in the header file, and θl_{oc} is the local incidence angle, which is derived from the Geocoded Incidence Angle file.

There were many speckle noises in the original SAR images, which make the radiometric and textural aspects less efficient [13]. Hence, an adaptive speckle filter was applied. In this study, Lee filter [14], one of the most common adaptive filters, was used. The window size of Lee filter was set as 3×3, 5×5, 7×7, 9×9 and 11×11 pixels. When the window size was 3×3, 5×5 and 7×7 pixels, the speckle noises cannot be removed completely. However, when the window size was 11×11 pixels, the histogram would change much from the original image. Considering these and the size of buildings, the window size of Lee filter was set as 9×9 pixels (about 11 m×11 m), similar to a small building's size in this area.

IV. CHANGE DETECTION

After the image pre-processing, the three TerraSAR-X images in Sigma Naught, taken in different days, were used to detect urban changes in this period (1.5 years). Firstly, color composition was applied to see changed areas visually, shown in Fig. 2(d). The first image taken in May, 2008 is plotted in Red, the second image taken in October, 2008 is plotted in Green, and the third image taken in November, 2009 is plotted in Blue. From Fig. 2(d), the change areas were shown in color while the non-change areas were shown in gray. The progress of D-runway construction can be seen easily from the color composited image.

To detect these changes automatically, the difference of the backscattering coefficients and the correlation coefficient were derived from the three images. This method was employed by Matsuoka and Yamazaki [7] to detect changes due to natural disasters in urban areas. In our case, the same method was applied to urban changes in a normal time. The approach of change detection was shown in Fig. 3. The difference (d) was calculated by (2) and the correlation coefficient (r) was calculated by (3).

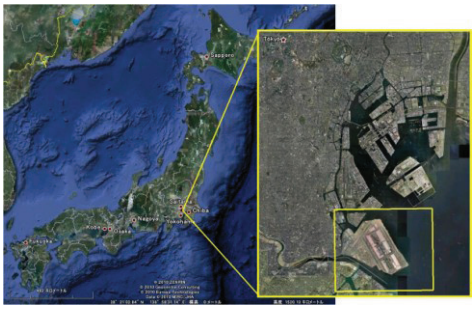

Figure 1. The study area of Tokyo International Airport, Japan.

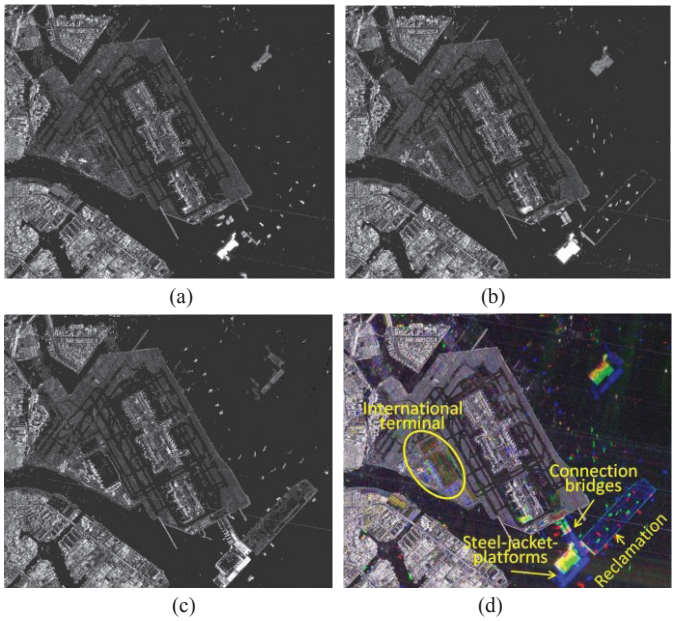

Figure 2. TerraSAR-X images taken on May 23th, 2008 (a), on Otc. 10th, 2008 (b), and on Nov. 23th, 2009 (c); (d) is a color composited image by (a-c) after image pre-processing as R: (a), G: (b), B: (c).

$$d = \bar{I}b_i - \bar{I}a_i \quad (2)$$

$$r = \frac{N\sum_{i=1}^{N} Ia_i Ib_i - \sum_{i=1}^{N} Ia_i \sum_{i=1}^{N} Ib_i}{\sqrt{\left(N\sum_{i=1}^{N} Ia_i^2 - \left(\sum_{i=1}^{N} Ia_i\right)^2\right) \cdot \left(N\sum_{i=1}^{N} Ib_i^2 - \left(\sum_{i=1}^{N} Ib_i\right)^2\right)}} \quad (3)$$

where i is the pixel number, Ia_i and Ib_i are the backscattering coefficient of the second (before) and first (after) images, $\bar{I}a_i$ and $\bar{I}bi$ are the corresponding averaged values over the N (= $k \times k$) pixels window surrounding the i-th pixel. In this study, the window size k is set as 9 pixels, the same as the speckle filter's.

A. Changes between May to October in 2008

The difference and the correlation coefficient between the first image taken on May 23th and the second image taken on Oct. 10th were calculated. In the resulted image of difference, the urban changes were shown by either negative or positive values. The negative change represents the reduction of reflection, which can be considered as removed buildings; the

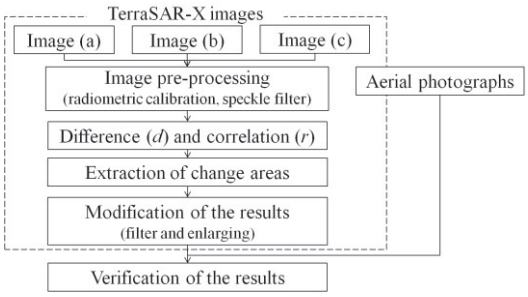

Figure 3. Flowchart of change detection from three temporal TerraSAR-X images.

positive change represents the increase of reflection, which can be considered as new constructions. The maximum change in the backscattering coefficient was about ±38 dB. In the resulted image of correlation, the low correlation value means a change. However, even there was no change, vegetation and water areas showed very low correlation since the reflection of them would change much depending on the wind condition. Hence, change detection using the correlation coefficient directly would include a lot of errors. Then a factor (z) calculated by (4), which combines the difference and the correlation coefficient, was introduced to represent changes generally.

$$z = \frac{|d|}{Max(|d|)} - c \cdot r \tag{4}$$

where $Max(|d|)$ is the maximum absolute value in the difference and c is the weight between the difference and the correlation coefficient, set from 0 to 1.0.

Since the correlation was very sensitive to subtle changes, it shows a low value even there was no big change. On the contrary, the normalized absolute value of the difference is relatively stable. Hence, in this study, the weight for the difference was set bigger than that for the correlation. When the weight c was set as 0.5, twice bigger for the normalized absolute difference, the interference by water was still too strong to separate changes from noises. When the weight c was set as 0.25, four times of correlation, the change areas showed high values than noises, shown in Fig. 4(a). Then in this study, c was determined as 0.25, and the value of the factor z was between -0.25 and 1.25. A high value means high possibility of change. A color composited image is shown in Fig. 5(a), where the first image is plotted in Red and the second image in Green & Blue. Then the red areas represent the negative change while the cyan areas representing the positive changes. Comparing the color composited image with the factor image, the changed areas can be seen easily by red color (a high value) from Fig. 4(a). According to the histogram of the z image, the mean value (μ) is 0.01 while the standard variation (σ) is 0.11. To keep the objectivity of the detected results, the threshold value was calculated by (5), using the mean value and standard deviation.

$$v = \mu + 2 \cdot \sigma \tag{5}$$

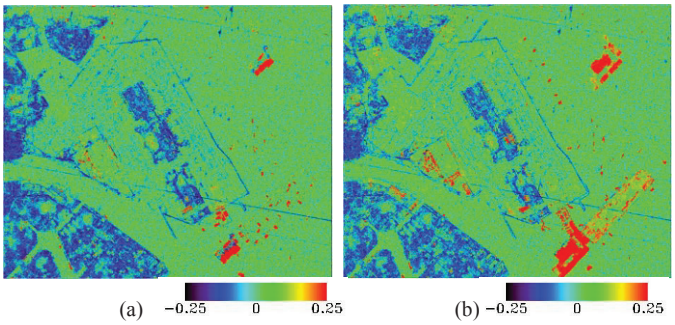

Figure 4. The change factor image calculated from the first and second images (a), and the second and third images (b).

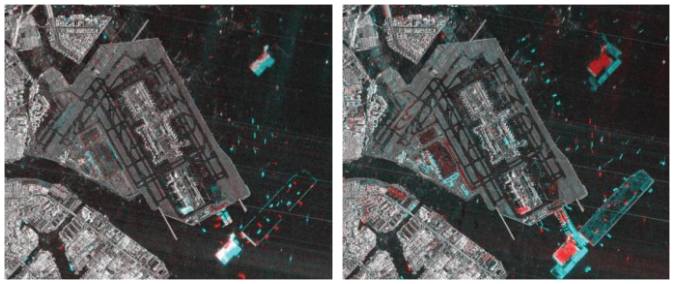

Figure 5. The color composited image as R: the first image, G&B: the second image (a) ; R: the second image, G&B: the third image (b).

In this case, the areas with value larger than 0.23 were extracted as changed areas. Then the extracted areas were overlapped on the result by the difference, to divide it into positive and negative changes. To remove noises from the detected result, a filter was applied. Considering the size of buildings and ships, the extracted areas which are smaller than 8×8 pixels (10 m×10 m) were removed as noises. Also a closing filter with the window size as 5×5 pixels was applied to keep the shape of the detected result more completely. Then the result of change detection was shown in Fig. 6(a), overlapping on an aerial photograph taken on May 20th, 2009. The negative changes were surrounded by red dashed lines, and the positive changes were surrounded by cyan solid lines. There were about 0.43 km^2 areas have positive changes while the negative constructions correspond to 0.29 km^2, including the changes of ambiguities.

B. Changes between October 2008 and November 2009

The difference and the correlation coefficient between the second image taken on Oct. 10th and the third image taken on Nov. 23th were also calculated to detect the changes. The maximum change in the backscattering coefficient between these images was about ±40 dB. Then the factor z was calculated from the difference and the correlation coefficient with the same weight, shown in Fig. 4(b). Comparing with the color composited image shown in Fig. 5(b), the changed areas on D-runway were matched with the red area in Fig. 4(b). According to the histogram of the z image, the mean value was 0.02 while the standard variation was 0.12. Therefore, the areas with value larger than 0.27 were extracted as changed areas. After filtering noises and applying the closing filter, the result of change detection was shown in Fig. 6(b), overlapping on the

(a) (b)

Figure 6. The part of detected results overlapping on the aerial photograph taken on May 20th, 2009.

aerial photograph. There were about 0.74 km^2 areas with positive changes while the negative changes correspond to 0.42 km^2, also including the changes due to ambiguity.

V. VERIFICATION

A manual (visual) detection was applied using the color composited images shown in Fig. 5 and the aerial photograph, to verify the accuracy. About 4.0 km^2 areas around the D-runway's location were selected as the sample area. Comparing the first and the second TerraSAR-X images manually, about 0.23 km^2 areas were detected as the positive changes, including the changes of ships; about 0.09 km^2 areas were detected as negative changes. Usually, the positive changes in urban areas represent newly built areas, and negative changes were removed building areas. In this area, most of the negative changes occurred due to slab installation for the runway. The surface of the slab was smooth with low backscatter for SAR, while the jackets before the slab installation show very high backscatter. From the second and the third TerraSAR-X images, about 1.20 km^2 areas were detected as positive changes and 0.24 km^2 areas were detected as negative changes visually. The comparisons of automatically detected results and manually detected results are shown in Tables I and II. The overall accuracy from the first and second images was 97%, and from the second and third images was 76%. The decrease of accuracy occurred due to the omission of the positive changes. Since the reclamation part of D-runway shows low backscatter of SAR, similar as the sea, this area cannot be detected automatically.

VI. CONCLUSIONS

In this study, the progress of HND expansion construction was monitored from three TerraSAR-X images, by a new factor combining the difference and the correlation coefficient. The manual detection was applied according to the color composition of two temporal TerraSAR-X images and an aerial photograph, to verify the accuracy. Almost all the changes due to the construction can be detected correctly by the proposed method. In the future, more examples will be carried to improve the method. This method can be a powerful tool to monitor urban development for a long time.

ACKNOWLEDGMENT

The TerraSAR-X images used in this study were made available from SAR Application Research Committee, organized by PASCO Corporation, Tokyo, Japan.

TABLE I. ACCURACY OF CHANGE DETECTION FROM THE FIRST AND SECOND IMAGES

		Manually detected results				
		Positive changes	*Negative changes*	*No change*	*Sum*	*User accuracy*
Automatically detected result	*Positive changes*	113,406	63	22,335	135,804	83.5%
	Negative changes	801	48,034	16,923	65,758	73.0%
	No change	33,523	7,332	2,275,499	2,316,354	98.2%
	Sum	147,730	55,429	2,314,757	2,517,916	
	Producer accuracy	76.8%	86.7%	98.3%		96.8%

TABLE II. ACCURACY OF CHANGE DETECTION FROM THE SECOND AND THIRD IMAGES

		Manually detected results				
		Positive changes	*Negative changes*	*No change*	*Sum*	*User accuracy*
Automatically detected result	*Positive changes*	228,155	133	28,718	257,006	88.8%
	Negative changes	553	120,371	5,551	126,475	95.2%
	No change	541,878	33,565	1,558,992	2,134,435	73.0%
	Sum	770,586	154,069	1,593,261	2,517,916	
	Producer accuracy	29.6%	78.1%	97.8%		75.8%

REFERENCES

[1] H. -P. Bahr, "Image segmentation for change detection in urban environments", Remote sensing and urban analysis, London: Taylor and Francis, Chap. 6, 2001, pp. 95-114.

[2] J. -P. Donnay, "Use of remote sensing information in planning", Geographic information and planning, Berlin: Springer, Chap. 13, 1997, pp. 242-260.

[3] C. Weber, "Urban agglomeration delimitation using remote sensing data, Remote sensing and urban analysis", Chap. 8, 2001, pp. 145-160.

[4] Y. Dong, B. Forster, and C. Ticehurst, "Radar backscatter analysis for urban environment", International Journal of Remote Sensing, Vol. 18, No. 6, 1997, pp. 135-1364.

[5] E. -M. Rignot, and J. J. Van Zyl, "Change detection techniques for ERS-1 SAR data", IEEE Transactions on Geoscience and Remote Sensing, Vol. 31, No. 4, 1993, pp. 896-906.

[6] M. Matsuoka, and F. Yamazaki, "Interferometric characterization of areas damaged by the 1995 Kobe earthquake using satellite SAR images", In: Proceedings of the 12th World Conferenceon Earthquake Engineering, ID2141, 2000.

[7] M. Matsuoka, and F. Yamazaki, "Use of satellite SAR intensity imagery for detecting building areas damaged due to earthquakes", Earthquake Spectra, Vol. 20, No. 3, 2004, pp. 975-994.

[8] C. Yonezawa, and S. Takeuchi, "Detection of urban damage using interferometric SARdecorrelation", In: Proceedings of International Geoscience and Remote Sensing Symposium, Institute of Electrical and Electronics Engineers, 1999, pp. 925–927.

[9] HANEDA Airport Construction Office, "HANEDA D-Runway report".

[10] Infoterra, "TerraSAR-X Services - Image Product Guide".

[11] F. K. Li and W. –K. Johnson, "Ambiguities in spaceborne synthetic aperture radar systems", IEEE Transactions on Aerospace and Electronic Systems, Vol. 19, 1983, pp. 389-396.

[12] Infoterra, "Radiometric Calibration of TerraSAR-X Data: Beta Naught and Sigma Naught Coefficient Calculation".

[13] A. Lopes, R. Touzi, and E. Nezry, "Adaptive speckle filters and Scene Heterogenteity", IEEE Transcations on Geoscience and Remote Sensing, Vol. 28, No. 6, 1990, pp. 992-1000.

[14] J. S. Lee, "Digital image enhancement and noise filtering by use of local statistics", IEEE Transactions on Pattern Analysis and Machine Intelligence, 1980, pp. 165–168.